



## Thermocatalytic analysis of CO<sub>2</sub>-CO selective chemisorption mechanism on lithium cuprate (Li<sub>2</sub>CuO<sub>2</sub>) and oxygen addition effect



Ana Yañez-Aulestia<sup>a</sup>, J. Francisco Gómez-García<sup>a</sup>, J. Arturo Mendoza-Nieto<sup>a</sup>, Yuhua Duan<sup>b</sup>, Heriberto Pfeiffer<sup>a,\*</sup>

<sup>a</sup> Laboratorio de Fisicoquímica y Reactividad de Superficies (LaFREs), Instituto de Investigaciones en Materiales, Universidad Nacional Autónoma de México, Circuito Exterior s/n, Cd. Universitaria, Del. Coyoacán, C.P. 04510, Ciudad de México, Mexico

<sup>b</sup> National Energy Technology Laboratory, United States Department of Energy, 626 Cochrans Mill Road, Pittsburgh, PA, 15236, United States

### ARTICLE INFO

#### Keywords:

CO<sub>2</sub> chemisorption  
CO oxidation  
Selective sorption process  
Lithium cuprate

### ABSTRACT

In the present work, thermogravimetric and catalytic analyses were performed in order to evidence the chemisorption selective mechanism followed during the CO and CO<sub>2</sub> chemisorption processes on Li<sub>2</sub>CuO<sub>2</sub> under different atmosphere conditions. Results were contrasted with some thermodynamic data. According to TG results, when the gas flow was composed by one gas (CO or CO<sub>2</sub>), chemisorption occurred through a superficial reaction followed by a volumetric capture. In the CO case, a double process was produced; CO oxidation and subsequent CO<sub>2</sub> chemisorption. Here, Li<sub>2</sub>CuO<sub>2</sub>, initially, catalyzed the CO oxidation and then it sorbed CO<sub>2</sub>. However, as Li<sub>2</sub>CuO<sub>2</sub> structure and composition evolves, it could not be strictly considered as a catalyst. On the other hand, when both gases were present (CO-CO<sub>2</sub>), a chemisorption competition was observed as a function of temperature, where CO was always selectively chemisorbed. Furthermore, O<sub>2</sub> presence modified positively the chemisorption abilities in binary (CO-O<sub>2</sub> and CO<sub>2</sub>-O<sub>2</sub>) and ternary (CO-CO<sub>2</sub>-O<sub>2</sub>) gas systems, in comparison with analogous tests performed in absence of O<sub>2</sub>.

### 1. Introduction

In the last two decades, several papers have reported the CO<sub>2</sub> capture on different materials [1–5], due to the threatening environmental situation. In that sense, alkaline ceramics seem to present good CO<sub>2</sub> sorption properties, mainly at high temperatures (300 ≤ T ≤ 850 °C) [1,6–19]. These alkaline ceramics are able to trap CO<sub>2</sub> chemically, through a double chemisorption process produced at surface and bulk particle sections [20]. The initial reaction process, superficial chemisorption, is produced by an acid-base reaction mechanism as alkaline ceramics present high basic characteristics. On the contrary, CO<sub>2</sub> is an acid molecule, which according to the Lux and Flood acid-base theory [21,22] is able to accept an oxygen anion from the basic component; the alkaline crystal structure in this case, producing CO<sub>3</sub><sup>2-</sup>. Moreover, as oxygen diffusion is needed to complete the carbonation process of alkaline ceramics, different authors have evidenced the positive effect produced by oxygen addition, where CO<sub>2</sub> and O<sub>2</sub> adsorption competition has been described during the superficial chemisorption process [23–25].

On the other hand, it was recently published that some alkaline ceramics (Li<sub>2</sub>CuO<sub>2</sub>, Li<sub>5</sub>FeO<sub>4</sub>, NaCoO<sub>2</sub> and Na<sub>2</sub>ZrO<sub>3</sub>) are able to

chemisorb carbon monoxide (CO), through a CO oxidation and subsequent CO<sub>2</sub> chemisorption process [26–28]. In these cases, CO capture process follows a similar superficial and bulk chemisorption mechanism than that described above for CO<sub>2</sub>, once CO has been previously oxidized. Such bifunctional application may be of great interest for developing gas separation systems. In that sense, there are several kinds of gas mixtures, such as syngas or biogas [29], where CO and/or CO<sub>2</sub> separation would modify or produce different gas compositions for final applications. For example, there are some biogas or syngas compositions where the amounts of CO<sub>2</sub> and CO are large and similar to methane (CH<sub>4</sub>) or hydrogen (H<sub>2</sub>) concentrations. In these cases, carbon oxides separation would be ideally desired, in order to obtain gas mixtures with larger heat capacities.

It should be mentioned that lithium cuprate (Li<sub>2</sub>CuO<sub>2</sub>) has shown some interesting CO<sub>2</sub> and CO capture properties [30–36], although it has not been largely studied. Li<sub>2</sub>CuO<sub>2</sub> has an orthorhombic crystalline structure (a = 3.655 Å, b = 2.860 Å, c = 9.377 Å and Z = 2, [37]), where lithium atoms are located between the (CuO<sub>4</sub>)<sup>2-</sup> square layers. In the Li<sub>2</sub>CuO<sub>2</sub> crystalline structure, lithium atoms have a high diffusion capacity. Moreover, it has to be mentioned that copper is able to change its oxidation state releasing oxygen, which enhances CO<sub>2</sub> and CO

\* Corresponding author.

E-mail address: [pfeiffer@iim.unam.mx](mailto:pfeiffer@iim.unam.mx) (H. Pfeiffer).

capture properties, in comparison to other alkaline ceramics.

Based on that, the aim of this work was to analyze the CO<sub>2</sub> and CO selective sorptions on lithium cuprate, one of the most promising alkaline ceramics for CO<sub>2</sub> chemisorption and CO oxidation-chemisorption processes. Thus, different catalytic and thermogravimetric analyses were conducted as an initial approximation for understanding the reaction mechanism. This analysis was performed in presence and absence of oxygen.

## 2. Experimental section

Li<sub>2</sub>CuO<sub>2</sub> ceramic was synthesized by solid-state reaction as it was previously reported in literature [31,35]. Lithium (Li<sub>2</sub>O, Aldrich, 99%) and copper (CuO, Meyer, 97%) oxides were used as reagents, mechanically mixed and then calcined in air atmosphere at 800 °C for 6 h. 20 wt% of lithium oxide excess was added in order to compensate Li sublimation at  $T > 720$  °C [37–39]. After, powder X-ray diffraction (XRD) was used to confirm the formation of Li<sub>2</sub>CuO<sub>2</sub> crystalline phase (data not shown). Moreover, some microstructural characteristics of Li<sub>2</sub>CuO<sub>2</sub> were determined by N<sub>2</sub> adsorption-desorption analysis in a Bel-Japan Minisorp II equipment at 77 K. Prior to analysis, the sample was degassed at room temperature for 12 h in vacuum. Finally, the BET model was used to determine the specific surface area ( $S_{\text{BET}} = 1.9 \text{ m}^2/\text{g}$ ).

Carbon monoxide (CO) and carbon dioxide (CO<sub>2</sub>) chemisorption capabilities were evaluated simultaneously in a TA Instruments Q500 thermobalance (~50 mg of sample) and in a catalytic reactor (Bel-Japan, model Bel-Rea, 200 mg of sample). In both analyses, samples were dynamically heated from 30 to 900 °C at 2 °C/min, using 4 mL/min of each gas in the following atmospheres: i) CO<sub>2</sub> (Praxair, grade 3.0), ii) CO (5 vol% in N<sub>2</sub>, Praxair certificate standard), iii) CO-CO<sub>2</sub>, iv) CO-O<sub>2</sub> (Praxair, grade 2.6), v) CO<sub>2</sub>-O<sub>2</sub> and vi) CO-CO<sub>2</sub>-O<sub>2</sub>, all diluted in N<sub>2</sub> to complete 100 mL/min. In TG analysis (Q500HR, from TA Instruments), chemisorption-desorption processes were evaluated following changes in the sample weight; whereas in reactor analysis, gas products were analyzed with a GC-2014 gas chromatograph (Shimadzu) with a Carboxen-1000 column. Then, some isothermal experiments were performed with ~100 mg of sample at different selected temperatures (350, 550 and 700 °C). For isothermal tests, samples were heated rapidly from room temperature to specified temperature, using N<sub>2</sub> (40 mL/min) as carrier gas; once the desired temperature was achieved, the flow gas was switched to desired gas mixture (CO-CO<sub>2</sub> or CO-CO<sub>2</sub>-O<sub>2</sub>) during 3 h. Isothermal products were analyzed by powder XRD to identify the crystal phases produced by different atmospheres and temperature conditions. XRD patterns were recorded in the  $5^\circ \leq 2\theta \leq 80^\circ$  range, using a goniometer speed of  $0.02^\circ(2\theta)/\text{min}$ , with a Siemens D5000 diffractometer coupled to a cobalt anode ( $\lambda = 1.7889 \text{ \AA}$ ). Crystal phases were identified using the Joint Committee Powder Diffraction Standards (JCPDS).

Temperature programmed desorption (TPD) analyses were performed in a chemisorption analyzer (Belcat, Bel-Japan) with 50 mg of sample. Sample was pre-treated at 850 °C under a He flow (30 mL/min). The sample was then cooled to 200 °C and saturated with 5 mL/min of CO or CO<sub>2</sub>. In both cases, gases were diluted in N<sub>2</sub> up to 100 mL/min during 60 min. Afterwards, TPD analyses were carried out by heating the sample up to 900 °C at 2 °C/min, in a He flow, quantifying data with a thermal conductivity detector (TCD).

## 3. Results and discussion

In order to analyze the CO<sub>2</sub>-CO sorption mechanism on Li<sub>2</sub>CuO<sub>2</sub>, different thermogravimetric and catalytic experiments were performed using the following gas mixtures: CO<sub>2</sub>, CO, CO<sub>2</sub>-O<sub>2</sub>, CO-O<sub>2</sub>, CO<sub>2</sub>-CO and CO<sub>2</sub>-CO-O<sub>2</sub>. Initially, dynamic thermograms of CO<sub>2</sub> and CO gases, as well as the CO<sub>2</sub>-O<sub>2</sub> and CO-O<sub>2</sub> gas mixtures, are shown in Fig. 1. CO<sub>2</sub> and CO<sub>2</sub>-O<sub>2</sub> dynamic experiments presented the typical behavior

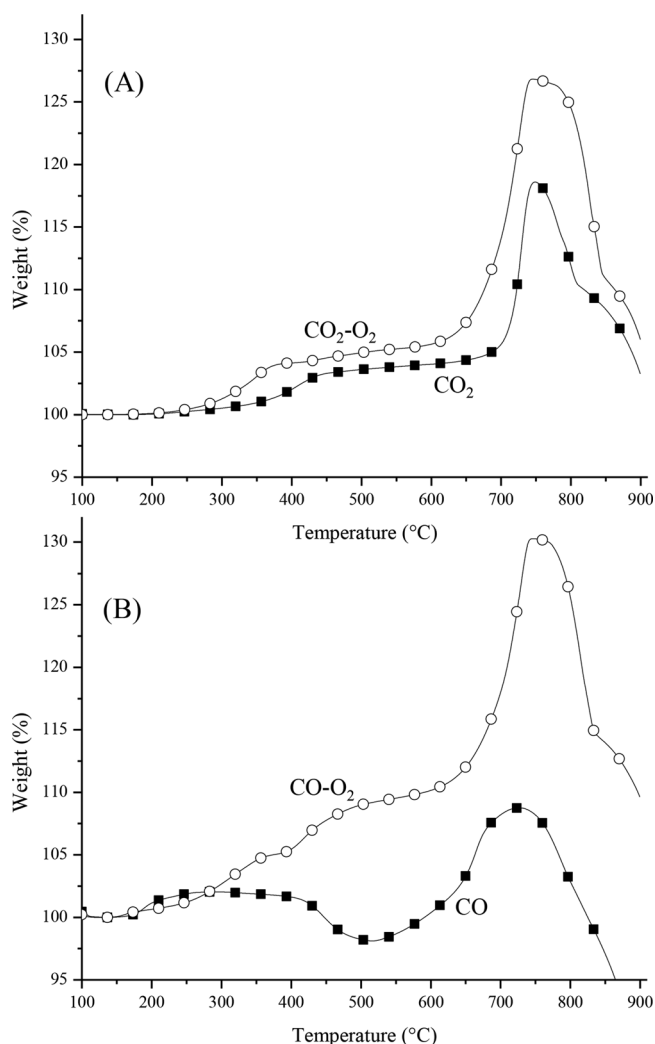


Fig. 1. Thermograms of Li<sub>2</sub>CuO<sub>2</sub> sample treated under different carbon oxide atmospheres: (A) CO<sub>2</sub> and CO<sub>2</sub>-O<sub>2</sub>, (B) CO and CO-O<sub>2</sub>.

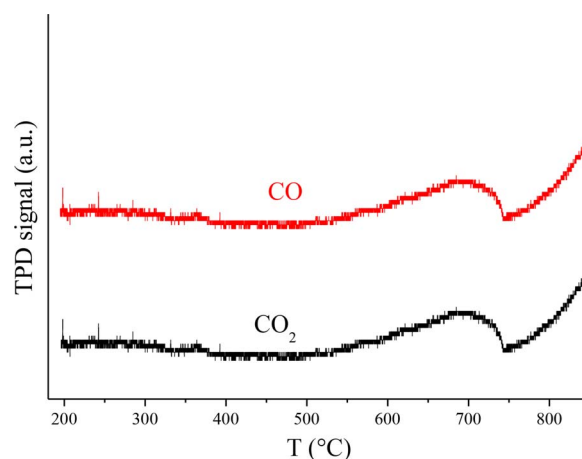


Fig. 2. Temperature programmed desorption of CO<sub>2</sub> or CO on Li<sub>2</sub>CuO<sub>2</sub>.

previously reported for Li<sub>2</sub>CuO<sub>2</sub> (Fig. 1A) [24,30,33–36]. For the CO<sub>2</sub> case, Li<sub>2</sub>CuO<sub>2</sub> presented an initial weight increment of 4 wt% between 350 and 600 °C, where superficial CO<sub>2</sub> chemisorption occurred, producing an external shell composed by lithium carbonate (Li<sub>2</sub>CO<sub>3</sub>) and copper oxide (CuO). Then, a second CO<sub>2</sub> chemisorption process was produced between 660 and 750 °C, where sample gained a total weight

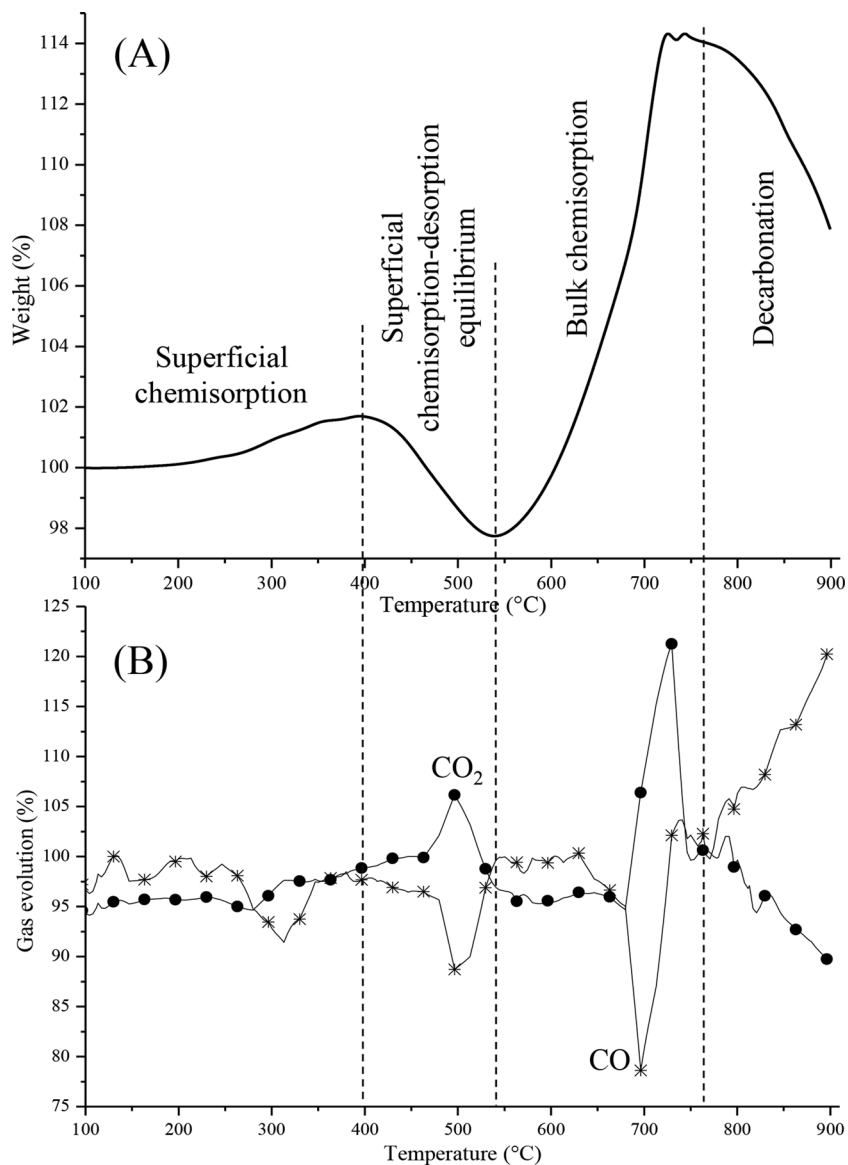


Fig. 3. Thermogravimetric profile (A) and catalytic evolution (B) of Li<sub>2</sub>CuO<sub>2</sub> sample treated on CO-CO<sub>2</sub> atmosphere.

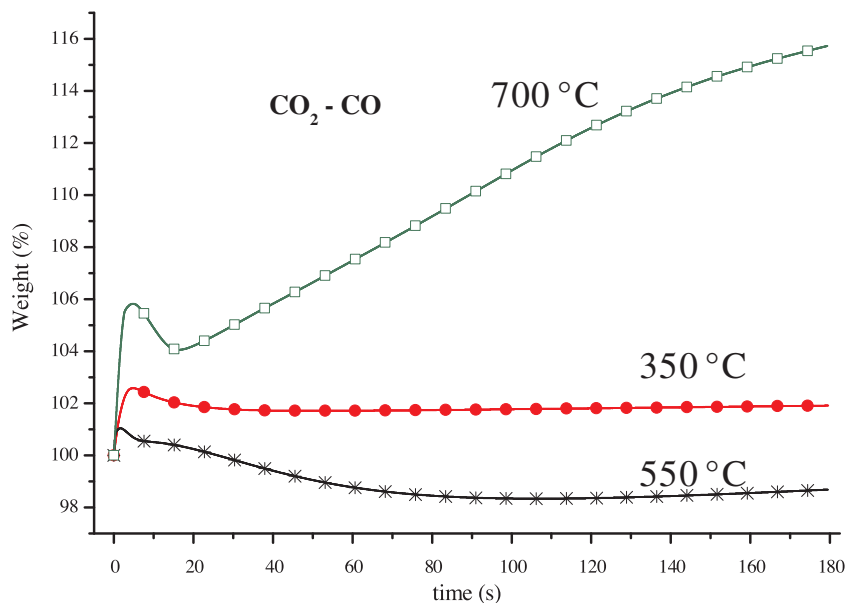


Fig. 4. Isothermal experiments for Li<sub>2</sub>CuO<sub>2</sub> sample tested using a CO<sub>2</sub>-CO atmosphere at different temperatures (350, 550 and 700 °C).

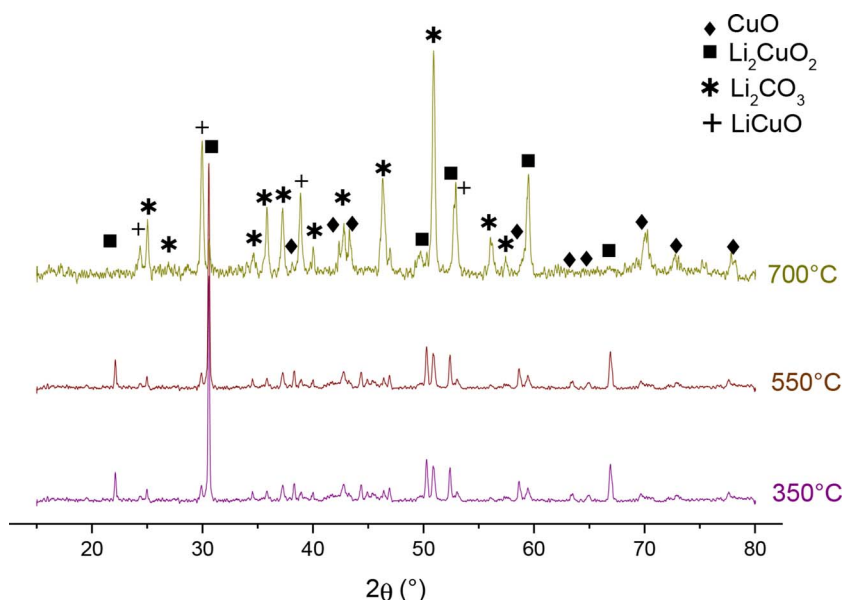
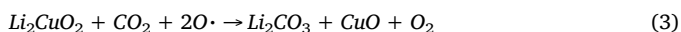


Fig. 5. XRD patterns for  $\text{Li}_2\text{CuO}_2$ -CO- $\text{CO}_2$  isothermal products obtained at different temperatures.

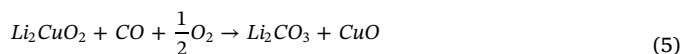
of 18.8 wt%. In this temperature range, lithium and oxygen diffusion processes are activated for  $\text{CO}_2$  bulk chemisorption (reaction (1)). Finally, at temperatures higher than  $750^\circ\text{C}$   $\text{CO}_2$  desorption was activated.  $\text{CO}_2$ - $\text{O}_2$  thermogram presented the same trend than that observed on the  $\text{CO}_2$  case, but oxygen addition improved  $\text{CO}_2$  superficial and bulk capture processes. In the  $\text{CO}_2$ - $\text{O}_2$  case, superficial and total (superficial + bulk)  $\text{CO}_2$  chemisorption were equal to 6 and 27 wt%, respectively. In a previous work, Lara-García et al. [24] showed that  $\text{CO}_2$  chemisorption is strongly enhanced by oxygen addition. When oxygen is supplied through the gas flow, copper atoms facilitate homolytic oxygen dissociation, where two free radical oxygen atoms are produced (reaction (2)). Then, dissociated oxygen atoms can be taken from the gas flow for carbonation without any crystalline diffusion process. Later, oxygen atoms, from  $\text{Li}_2\text{CuO}_2$  crystalline structure, can diffuse and release at any moment as oxygen molecules (reaction (3)).



In reaction (3),  $\text{O}^\bullet$  are the oxygen atoms taking part during the  $\text{Li}_2\text{CO}_3$  formation, while the  $\text{O}_2$  molecule, presented on the product side of this reaction, corresponds to the oxygen atoms diffused and released from the  $\text{Li}_2\text{CuO}_2$  crystalline structure.

Fig. 1B shows the CO and  $\text{CO}_2$ - $\text{O}_2$  dynamic thermograms. Both curves evidenced weight increments, which can be attributed to carbonation processes. In the CO case, the thermogram showed a weight increment (2.2 wt%) between 150 and  $320^\circ\text{C}$ , associated to CO superficial chemisorption. Then, between 320 and  $500^\circ\text{C}$  a superficial desorption was produced. At higher temperatures, a second weight increment was produced between 530 and  $720^\circ\text{C}$ , which can be attributed to CO bulk chemisorption process. In this case, CO is being trapped chemically and structural oxygen atoms are used to produce  $\text{Li}_2\text{CO}_3$ . Consequently, copper cations in  $\text{Li}_2\text{CuO}_2$  must be partially or totally reduced, as it is proposed in reaction (4). A similar behavior was already observed for  $\text{Li}_5\text{FeO}_4$ -CO system, where partial iron reduction was detected from  $\text{Fe}^{3+}$  to  $\text{Fe}^{2+}$  or even more to  $\text{Fe}^0$  [32]. On the contrary, when oxygen is added (reaction (5)), carbonation generates the same final products as those obtained during  $\text{Li}_2\text{CuO}_2$  carbonation using carbon dioxide. In fact, thermodynamic analysis shows that reaction (5) is favored over the double reaction process; CO oxidation and subsequent lithium

cuprate carbonation [27].



In the last case ( $\text{CO}$ - $\text{O}_2$ ), superficial (9 wt%) and bulk (30.5 wt%) weight increments were the highest among different gas mixtures analyzed. Thus,  $\text{Li}_2\text{CuO}_2$  is able to catalyze the conversion of CO to  $\text{CO}_2$  and chemisorbs the product, although  $\text{Li}_2\text{CuO}_2$  could not be established as a catalyst as it evolves chemically during the  $\text{CO}_2$  chemisorption process. Moreover,  $\text{Li}_2\text{CuO}_2$  chemical change modifies particle microstructural evolution, enhancing final  $\text{CO}_2$  chemisorption.

In order to verify if CO and  $\text{CO}_2$  sorption processes are produced at the same  $\text{Li}_2\text{CuO}_2$  active sites, TPD- $\text{CO}_2$  experiments were performed with both gases (Fig. 2). In both cases, the TPD curves showed two  $\text{CO}_2$  desorption processes at  $500$ – $750^\circ\text{C}$  and  $T > 750^\circ\text{C}$ . These processes can be associated to  $\text{CO}_2$  molecules strongly sorbed on  $\text{Li}_2\text{CuO}_2$  particles and  $\text{Li}_2\text{CuO}_2$  decarbonation process, respectively. It must be pointed out that TPD experiments presented exactly the same behavior, independently of the sorbed gas, CO or  $\text{CO}_2$ . Thus, sorption process and  $\text{Li}_2\text{CuO}_2$  superficial active sites are the same for CO and  $\text{CO}_2$ .

After  $\text{CO}_2$  and CO chemisorption evaluation on  $\text{Li}_2\text{CuO}_2$ , in presence and absence of oxygen,  $\text{CO}_2$ -CO and  $\text{CO}_2$ - $\text{CO}$ - $\text{O}_2$  systems were analyzed. In both cases, thermograms presented similar trends as those obtained previously. However, gas evolution was followed in order to determine whether  $\text{CO}_2$  or CO were selectively chemisorbed. On the  $\text{CO}_2$ -CO case (Fig. 3), thermogram showed four different sections; i) superficial chemisorption, ii) superficial chemisorption-desorption equilibrium, iii) bulk chemisorption and iv) decarbonation, where all these processes fit well to previous references on  $\text{Li}_2\text{CuO}_2$  [31]. Initially, superficial chemisorption process was observed between 250 and  $400^\circ\text{C}$ , with a weight increment of 1.9 wt% (Fig. 3A). In the same temperature range, gas evolution analysis did not evidence which carbon oxide would be associated to superficial chemisorption, although CO evolution suggested a partial consumption at around  $320^\circ\text{C}$  (Fig. 3B). At higher temperatures ( $400$ – $540^\circ\text{C}$ ), a superficial desorption was produced, inducing a chemisorption-desorption equilibrium. In this temperature range, gas evolution curve clearly showed CO consumption and  $\text{CO}_2$  production. Thus,  $\text{Li}_2\text{CuO}_2$  must be catalyzing CO to  $\text{CO}_2$ , but it is not trapped, as  $\text{CO}_2$  is detected in excess. Moreover,  $\text{CO}_2$  detection must be a consequence of CO oxidation and  $\text{CO}_2$  desorption. Once the bulk chemisorption is activated ( $T > 540^\circ\text{C}$ ), this thermogram showed an

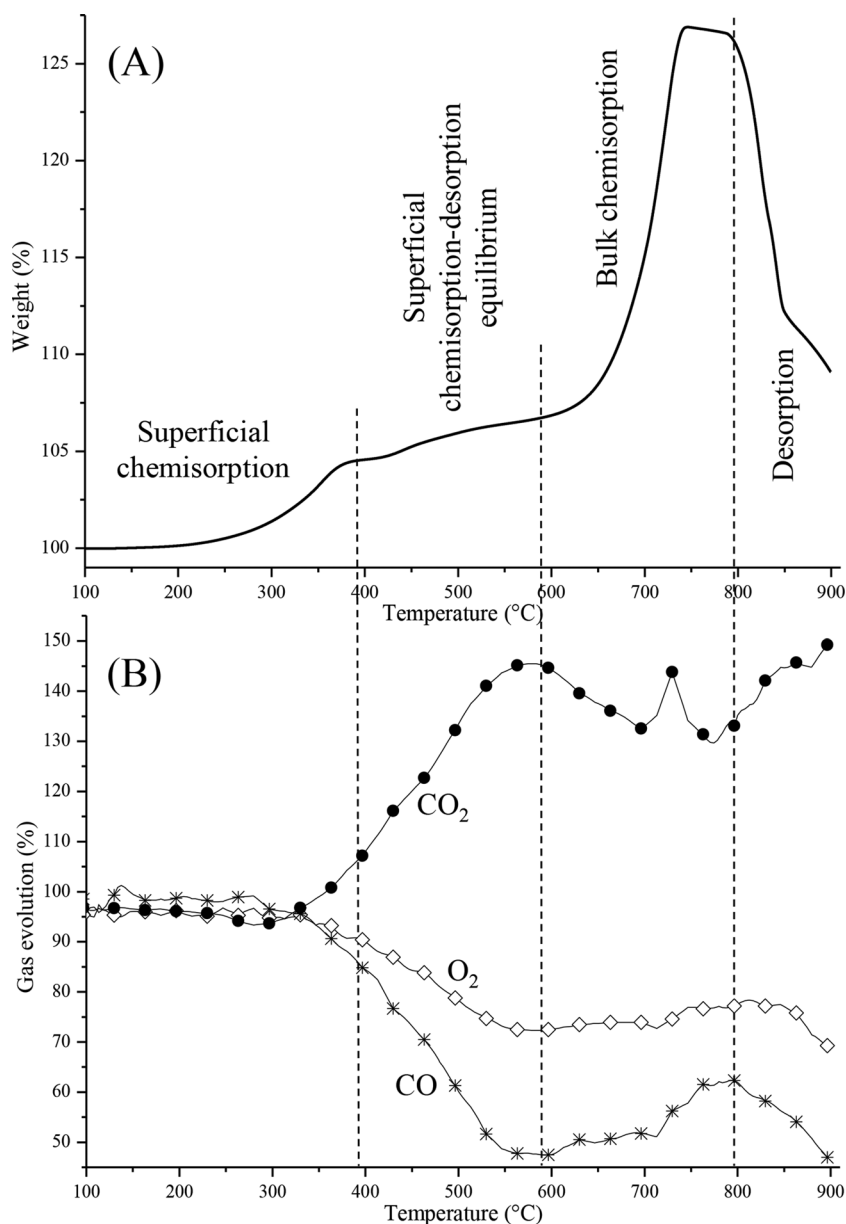


Fig. 6. Thermogravimetric profile (A) and catalytic evolution (B) of  $\text{Li}_2\text{CuO}_2$  sample treated on  $\text{CO-CO}_2\text{-O}_2$  atmosphere.

important weight increment of 14.7 wt%. At the same time, gas evolution curve shows that CO is consumed, while  $\text{CO}_2$  is being produced. These results show that CO is the gas consumed, where part of it is used for bulk chemisorption and the other part is only oxidized to  $\text{CO}_2$ . Therefore, in the  $\text{CO}_2\text{-CO}$  system, CO seems to be the most reactive specie, where the carbonation process must follow the reaction (4). In fact, the metallic copper production explains the last process; decarbonation. In this case,  $\text{CO}_2$  is consumed while CO is produced. Here,  $\text{CO}_2$  is partially reduced, producing a CO excess (between 760 and 900 °C), through copper re-oxidation or  $\text{Li}_2\text{CuO}_2$  regeneration.

In order to further analyze the  $\text{Li}_2\text{CuO}_2\text{-CO}_2\text{-CO}$  reaction mechanism, three specific isothermal experiments were performed at 350, 550 and 700 °C to represent superficial chemisorption, superficial chemisorption-desorption and bulk chemisorption processes, respectively. Moreover, isothermal products were analyzed by XRD to determine composition and structural changes produced by CO and  $\text{CO}_2$  chemisorption-desorption. Fig. 4 shows  $\text{Li}_2\text{CuO}_2\text{-CO}_2\text{-CO}$  isotherms. The isotherm performed at 350 °C showed an initial weight increment of 2.6 wt% after five minutes. This weight increment is similar to that observed in the dynamic experiment. After that, isotherm tends to reach

a chemisorption-desorption equilibrium, stabilizing the weight gained in 1.8 wt%. Final weight increment and temperature correspond to a superficial process. Then, isotherm performed at 550 °C chemically increased its weight by only 1.1 wt% after three minutes. After that, isotherm desorbed even more weight than that present at the beginning of this isotherm. This weight should be correlated to continuous CO oxidation process evidenced on the gas evolution curve (Fig. 3B). In this case, part of oxygen atoms, present into the  $\text{Li}_2\text{CuO}_2$  crystalline structure, are released to react with CO; producing  $\text{CO}_2$ . Thus,  $\text{Li}_2\text{CuO}_2$  should be partially decomposed through copper reduction. Finally, when isotherm was performed at 700 °C, an initial weight increment was observed (5.8 wt%) after five minutes, which corresponds to superficial chemisorption process. Then, superficial chemisorption-desorption and bulk chemisorption are activated, reaching a final weight increment of 15.8 wt%. As in the previous case (550 °C), chemisorption process must be produced through the copper reduction, according to thermogravimetric and gas evolution results (see Fig. 3). In order to probe this reaction mechanism, isothermal products were analyzed by powder XRD (Fig. 5). As it could be expected, X-ray diffraction patterns of isothermal products obtained at 350 and 550 °C mainly depicted the

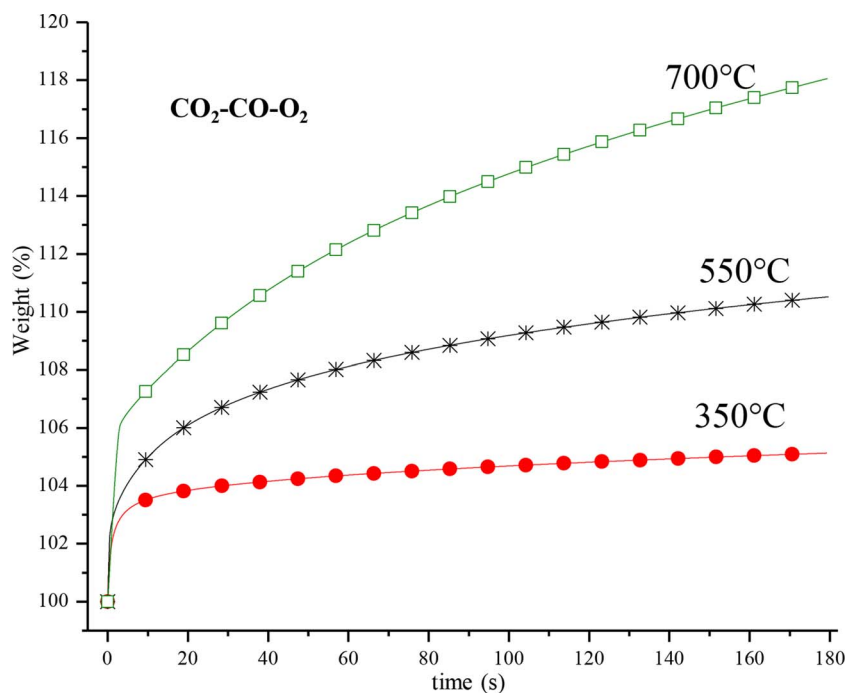


Fig. 7. Isothermal experiments for  $\text{Li}_2\text{CuO}_2$  sample tested using a  $\text{CO}_2\text{-CO-O}_2$  atmosphere at different temperatures (350, 550 and 700 °C).

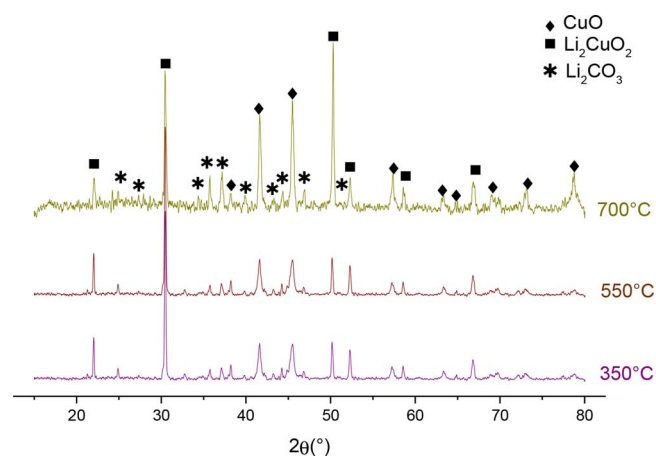
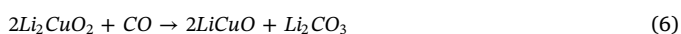


Fig. 8. XRD patterns of  $\text{Li}_2\text{CuO}_2\text{-CO-CO}_2\text{-O}_2$  isothermal products obtained at different temperatures.

presence of  $\text{Li}_2\text{CuO}_2$  (PDF file 01-084-1971) and  $\text{Li}_2\text{CO}_3$  (PDF file 00-022-1141) as the main carbonation product. Nevertheless, it was possible to determine the presence of a different lithium cuprate phase:  $\text{LiCuO}$  (PDF file 00-077-1698), where copper cations present a different oxidation state ( $\text{Cu}^{1+}$ ) from that presented on  $\text{Li}_2\text{CuO}_2$  ( $\text{Cu}^{2+}$ ). XRD pattern of isotherm performed at 700 °C confirmed the formation of  $\text{Li}_2\text{CO}_3$  and  $\text{LiCuO}$ , while  $\text{Li}_2\text{CuO}_2$  phase tended to disappear. Finally,  $\text{CuO}$  (PDF file 00-045-0937) was also detected in the last XRD pattern, which implies a partial reaction of copper element or a different carbonation reaction mechanism. These results confirmed the carbonation process, in which part of the oxygen atoms present in the  $\text{Li}_2\text{CuO}_2$  crystal phase are released to react with  $\text{CO}$ , producing the final carbonation process. However, the presence of small amounts of  $\text{CuO}$  confirmed that, at least, a small proportion of the carbonation process is produced by the direct  $\text{CO}_2$  chemisorption (reaction (1)). On the contrary, released oxygen (from  $\text{Li}_2\text{CuO}_2$  crystal structure) induces a partial copper reduction, according to following reaction (reaction (6)).



After the  $\text{CO}_2\text{-CO}$  system analysis, oxygen was included ( $\text{CO}_2\text{-CO-}$

$\text{O}_2$ ) in order to determine variations. Fig. 6 shows the same four chemisorption-desorption sections described above. Initially, superficial chemisorption was produced between 250 and 390 °C, producing a weight increment of 4.6 wt% (Fig. 6A). In this temperature range, gas evolution analysis showed that  $\text{CO}$  and  $\text{O}_2$  are consumed, while  $\text{CO}_2$  concentration increased (Fig. 6B). The same gas evolution tendency continued between 390 and 580 °C (superficial chemisorption-desorption equilibrium). Thus, as in the  $\text{CO}_2\text{-CO}$  system,  $\text{Li}_2\text{CuO}_2$  must catalyze  $\text{CO}$  to  $\text{CO}_2$  (reaction (7)), but  $\text{CO}_2$  is not highly chemisorbed as its weight only increased in 2.2 wt%. However, it should be mentioned that oxygen importantly modified the chemisorption-desorption equilibrium in this temperature range, in comparison to  $\text{CO}_2\text{-CO}$  system. Once bulk chemisorption is activated ( $T > 600$  °C), thermogram showed a total weight increment of 26.9 wt%, which is almost twice higher than that observed on  $\text{O}_2$  absence (Fig. 3A). In the same temperature range, gas evolution curve shows that  $\text{CO}$  is consumed as well as  $\text{O}_2$ , while  $\text{CO}_2$  increased. In fact, it can be seen that  $\text{CO}_2$  concentration presented the highest production at around 730 °C. Finally, at  $T \geq 800$  °C decarbonation process was evidenced, with the consequent  $\text{CO}$  and  $\text{O}_2$  consumptions and  $\text{CO}_2$  production, meaning that  $\text{CO}$  oxidation process continued in this temperature range.



As in the previous case, three isothermal experiments were performed (350, 550 and 700 °C) on the  $\text{Li}_2\text{CuO}_2\text{-CO}_2\text{-CO-O}_2$  system. Fig. 7 shows that isotherms presented an exponential behavior, where the final weights increased as a function of temperature. Isotherm performed at 350 °C presented a weight increment of 5.1 wt% after five minutes. This weight increment was higher than that observed on oxygen absence (2.1 wt%, see Fig. 4). At 550 and 700 °C, the total weight increments were 10.6 and 18.0 wt%, respectively. As in the lowest temperature (350 °C), oxygen addition favored the carbonation process, independently of temperature. Isothermal products were analyzed by XRD (Fig. 8), and diffractograms only showed the presence of  $\text{Li}_2\text{CuO}_2$ , as unreacted material, and  $\text{Li}_2\text{CO}_3$  and  $\text{CuO}$  as carbonation products, according to reactions (3) or (5). It should be mentioned that in the oxygen presence, copper was not partially reduced.

Comparing these results with theoretical Gibbs free energy ( $\Delta G$ ), the following facts can be seen (Fig. 9): 1)  $\text{CO}_2$  capture is always higher

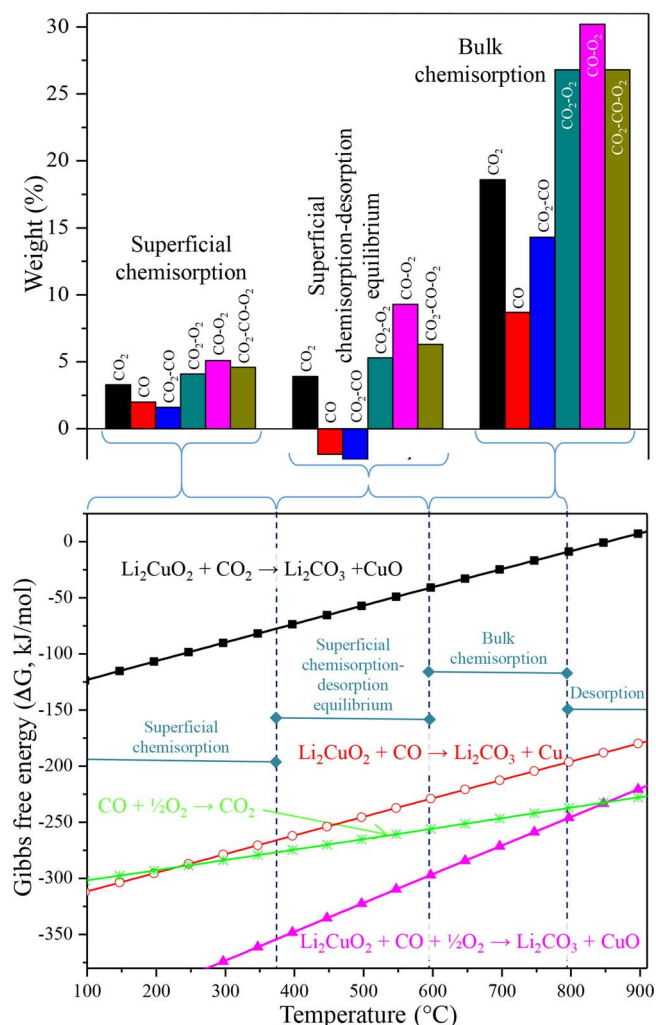


Fig. 9. Comparison between experimental data and theoretical calculations [27] for different  $\text{CO}_2$  and  $\text{CO}$  chemisorption-desorption processes occurred on  $\text{Li}_2\text{CuO}_2$ . Thermodynamic data was obtained for each reaction independently, and reaction data were presented to show which of them was the most suitable process at the different temperature ranges.

than that of  $\text{CO}$  at superficial chemisorption, superficial chemisorption-desorption equilibrium and bulk chemisorption temperature ranges, although the Gibbs free energies suggest a higher stability of  $\text{CO}$  chemisorption reaction. Therefore,  $\text{CO}$  chemisorption process must be slower, kinetically, than that of  $\text{CO}_2$ . It may be generated by oxygen release from  $\text{Li}_2\text{CuO}_2$  crystal structure producing lithium carbonate and  $\text{LiCuO}$ . 2) On the contrary, once oxygen is added, chemisorption of  $\text{CO}_2$  and  $\text{CO}$  are importantly improved. This result is in very good agreement with  $\Delta G$  values obtained for the  $\text{Li}_2\text{CuO}_2\text{-CO-O}_2$  system, which presents the highest thermodynamic stability. Moreover, from  $\Delta G$  data, it can be seen that at  $T < 845^\circ\text{C}$   $\text{CO}$  catalytic conversion to  $\text{CO}_2$  is less stable than  $\text{CO-O}_2$  chemisorption, confirming that  $\text{Li}_2\text{CuO}_2$  reaction with  $\text{CO}$  varies as a function of oxygen presence (reaction (5)) or absence (reaction (6)). 3) Finally, when  $\text{CO}_2$  and  $\text{CO}_2\text{-CO}$  systems are compared, all chemisorption processes decreased on the  $\text{CO}_2\text{-CO}$  case in oxygen absence, but enhanced in the presence of oxygen. As it could be expected, in oxygen absence,  $\text{CO}_2$  presence on  $\text{CO}_2\text{-CO}$  mixture must modify the  $\text{CO}$  catalytic conversion to  $\text{CO}_2$ , according to Le Chatelier's equilibrium law, reducing the chemisorption process due to low  $\text{CO}_2$  partial pressure in addition to the oxygen release necessity. On the contrary, once oxygen is added, reaction mechanism changes and  $\text{CO}$  oxidation (reaction (7)) is not the preponderant reaction.

#### 4. Conclusions

$\text{Li}_2\text{CuO}_2$  was synthesized and then tested for  $\text{CO}$  and  $\text{CO}_2$  chemisorption processes on presence or absence of  $\text{O}_2$ . Based on the results obtained, it was possible to establish different reaction mechanisms for each gas condition. Reaction mechanisms were corroborated through thermodynamic calculations ( $\Delta G$ ). According to TG experiments,  $\text{CO}_2$  chemisorption process was achieved using  $\text{Li}_2\text{CuO}_2$  as chemical sorbent (18.8 wt%) in a wide temperature range ( $400\text{--}750^\circ\text{C}$ ). This effect was significant enhanced by  $\text{O}_2$  addition; especially during bulk chemisorption stage (27.0 wt%, between  $600$  and  $800^\circ\text{C}$ ), where lithium and oxygen diffusion processes are active. Regarding to  $\text{CO}$  oxidation reaction, it can be established that it is slower than  $\text{CO}_2$  chemisorption on  $\text{O}_2$  absence, but it is highly enhanced by  $\text{O}_2$  addition ( $\text{CO-O}_2$ ). In the  $\text{CO}$  cases, it always presented a higher selectivity chemisorption on  $\text{Li}_2\text{CuO}_2$  than  $\text{CO}_2$ . Moreover, a bifunctional process took place during the  $\text{CO}$  chemisorption: 1)  $\text{CO}$  oxidation to  $\text{CO}_2$  and 2)  $\text{CO}_2$  chemisorption. According to all these results,  $\text{CO-O}_2$  system is the best condition for obtaining the highest chemical capture, among all gas compositions tested. Thus, oxygen addition avoids direct carbon monoxide chemisorption observed in  $\text{O}_2$  absence, while it significantly enhances the following processes; superficial chemisorption ( $\sim 5$  wt%), superficial chemisorption-desorption equilibrium ( $\sim 10$  wt%) and bulk adsorption ( $\sim 30$  wt%).

#### Acknowledgements

A. Yañez-Aulestia, J. A. Mendoza-Nieto and J. F. Gómez-García thank to CONACYT, SENER and DGAPA UNAM for personal financial support, respectively. The present work was financially supported by SENER-CONACYT (251801) and PAPIIT-UNAM (IN-101916) projects. Finally, authors thank to Adriana Tejeda and Alberto Lopez for technical assistant.

#### References

- [1] L.K.G. Bhatta, S. Seetharamu, S. Oliviera, Lithium ceramics for high temperature  $\text{CO}_2$  capture: a review, *J. CPRI* 10 (2014) 395–408.
- [2] S. Choi, J.H. Drese, C.W. Jones, Adsorbent materials for carbon dioxide capture from large anthropogenic point sources, *ChemSusChem* 2 (2009) 796–854.
- [3] S.Y. Lee, S.J. Park, A review on solid adsorbents for carbon dioxide capture, *J. Ind. Eng. Chem.* 23 (2009) 1–11.
- [4] M. Olivares-Marín, T.C. Drage, M.M. Maroto-Valer, Novel lithium-based sorbents from fly ashes for  $\text{CO}_2$  capture at high temperatures, *Int. J. Greenh. Gas Control* 4 (2013) 623–629.
- [5] Q. Wang, J. Luo, Z. Zhong, A. Borgna,  $\text{CO}_2$  capture by solid adsorbents and their applications: current status and new trends, *Energy Environ. Sci.* 4 (2011) 42–55.
- [6] T.L. Ávalos-Rendón, H. Pfeiffer, High  $\text{CO}_2$  chemisorption in  $\alpha\text{-Li}_5\text{AlO}_4$  at low temperatures ( $30\text{--}80^\circ\text{C}$ ): effect of the water vapor addition, *Energy Fuels* 26 (2012) 3110–3314.
- [7] X. Guo, L. Ding, J. Ren, H. Yang, Preparation and  $\text{CO}_2$  capture properties of nanocrystalline  $\text{Li}_2\text{ZrO}_3$  via an epoxide-mediated sol-gel process, *J. Sol-Gel Sci. Technol.* 81 (2017) 844–849.
- [8] S. Jeong, J.H. Lee, H.Y. Kim, H.R. Moon, Effects of porous carbon additives on the  $\text{CO}_2$  absorption performance of lithium orthosilicate, *Thermochim. Acta* 637 (2016) 31–37.
- [9] G. Ji, M.Z. Memon, H. Zhuo, M. Zhao, Experimental study on  $\text{CO}_2$  capture mechanisms using  $\text{Na}_2\text{ZrO}_3$  sorbents synthesized by soft chemistry method, *Chem. Eng. J.* 313 (2017) 646–654.
- [10] J.S. Lee, C.T. Yavuz, Enhanced sorption cycle stability and kinetics of  $\text{CO}_2$  on lithium silicates using lithium ion channeling effect of  $\text{TiO}_2$  nanotubes, *Ind. Eng. Chem. Res.* 56 (2017) 3413–3417.
- [11] W. Li, Z. Yin, Z. Zhou, P. Zhao, High-capacity  $\text{Li}_4\text{SiO}_4$ -based  $\text{CO}_2$  sorbents via a facile hydration-NaCl doping technique, *Energy Fuels* 31 (2017) 6257–6265.
- [12] A. Nambo, J. He, T.Q. Nguyen, V. Atla, T. Druffel, M. Sunkara, Ultrafast carbon dioxide sorption kinetics using lithium silicate nanowires, *Nano Lett.* 17 (2017) 3327–3333.
- [13] M. Seggiani, M. Puccini, S. Vitolo, Alkali promoted lithium orthosilicate for  $\text{CO}_2$  capture at high temperature and low concentration, *Int. J. Greenh. Gas Control* 17 (2013) 25–31.
- [14] P.V. Subha, B.N. Nair, P. Hareesh, A.P. Mohamed, T. Yamaguchi, K.G. Warrier, U.S. Hareesh,  $\text{CO}_2$  absorption studies on mixed alkali orthosilicates containing rare-earth second-phase additives, *J. Phys. Chem. C* 119 (2015) 5319–5326.
- [15] C. Wang, B. Dou, Y. Song, H. Chen, Y. Xu, B. Xie, High temperature  $\text{CO}_2$  sorption on  $\text{Li}_2\text{ZrO}_3$  based sorbents, *Ind. Eng. Chem. Res.* 53 (2014) 12744–12752.

- [16] K. Wang, Z. Yin, P. Zhao, Synthesis of macroporous  $\text{Li}_4\text{SiO}_4$  via a citric acid-based sol-gel route coupled with carbon coating and its  $\text{CO}_2$  chemisorption properties, *Ceram. Int.* 42 (2016) 2990–2999.
- [17] X. Yang, W. Liu, J. Sun, Y. Hu, W. Wang, H. Chen, Y. Zhang, X. Li, M. Xu, Alkali-doped lithium orthosilicate sorbents for carbon dioxide capture, *ChemSusChem* 9 (2016) 2480–2487.
- [18] Q. Zhang, D. Peng, S. Zhang, Q. Ye, Y. Wu, Y. Ni, Behaviors and kinetic models analysis of  $\text{Li}_4\text{SiO}_4$  under various  $\text{CO}_2$  partial pressures, *AIChE J.* 63 (2017) 2153–2164.
- [19] Z. Zhou, K. Wang, Z. Yin, P. Zhao, Z. Su, J. Sun, Molten  $\text{K}_2\text{CO}_3$ -promoted high-performance  $\text{Li}_4\text{SiO}_4$  sorbents at low  $\text{CO}_2$  concentrations, *Thermochim. Acta* (2017), <http://dx.doi.org/10.1016/j.tca.2017.07.014>.
- [20] J. Ortiz-Landeros, T.L. Ávalos-Rendón, C. Gómez-Yáñez, H. Pfeiffer, Analysis and perspectives concerning  $\text{CO}_2$  chemisorption on lithium ceramics using thermal analysis, *J. Therm. Anal. Calorim.* 108 (2012) 647–655.
- [21] H. Lux, G. Säuren, S. Basen, Die Bestimmung der Sauerstoffionen-Konzentration, *Z. Elektrochem.* 45 (1939) 303–309.
- [22] H. Flood, T. Førland, The acidic and basic properties of oxides, *Acta Chem. Scand.* 1 (1947) 592–604.
- [23] H.A. Lara-García, P. Sanchez-Camacho, Y. Duan, J. Ortiz-Landeros, H. Pfeiffer, Analysis of the  $\text{CO}_2$  chemisorption in  $\text{Li}_5\text{FeO}_4$ : a new high temperature  $\text{CO}_2$  captor material, *J. Phys. Chem. C* 121 (2017) 3455–3462.
- [24] H.A. Lara-García, H. Pfeiffer, High and efficient  $\text{Li}_2\text{CuO}_2$ - $\text{CO}_2$  chemisorption using different partial pressures and enhancement produced by the oxygen addition, *Chem. Eng. J.* 313 (2017) 1288–1294.
- [25] L. Martínez-dlCruz, H. Pfeiffer, Effect of oxygen addition on the thermokinetic properties of  $\text{CO}_2$  chemisorption on  $\text{Li}_2\text{ZrO}_3$ , *Ind. Eng. Chem. Res.* 49 (2010) 9038–9042.
- [26] B. Alcántar-Vázquez, Y. Duan, H. Pfeiffer,  $\text{CO}$  oxidation and subsequent  $\text{CO}_2$  chemisorption on alkaline zirconates:  $\text{Li}_2\text{ZrO}_3$  and  $\text{Na}_2\text{ZrO}_3$ , *Ind. Eng. Chem. Res.* 55 (2016) 9880–9886.
- [27] H.A. Lara-García, B. Alcántar-Vázquez, Y. Duan, H. Pfeiffer,  $\text{CO}$  chemical capture on lithium cuprate, through a consecutive  $\text{CO}$  oxidation and chemisorption bifunctional process, *J. Phys. Chem. C* 120 (2016) 3798–3806.
- [28] E. Vera, B. Alcántar-Vázquez, Y. Duan, H. Pfeiffer, Bifunctional application of sodium cobaltate as a catalyst and captor through  $\text{CO}$  oxidation and subsequent  $\text{CO}_2$  chemisorption processes, *RSC Adv.* 6 (2016) 2162–2170.
- [29] M.R. Stonor, T.E. Ferguson, J.G. Chen, A.H.A. Park, Biomass conversion to  $\text{H}_2$  with substantially suppressed  $\text{CO}_2$  formation in the presence of group I & group II hydroxides and a Ni/ZrO<sub>2</sub> catalyst, *Energy Environ. Sci.* 8 (2015) 1702–1706.
- [30] H.A. Lara-García, B. Alcántar-Vázquez, Y. Duan, H. Pfeiffer, Water steam effect during high  $\text{CO}_2$  chemisorption in lithium cuprate ( $\text{Li}_2\text{CuO}_2$ ) at moderate temperature: experimental and theoretical evidence, *RSC Adv.* 5 (2015) 34157–34165.
- [31] H.A. Lara-García, M.J. Ramírez-Moreno, J. Ortiz-Landeros, H. Pfeiffer,  $\text{CO}_2$  chemisorption in  $\text{Li}_2\text{CuO}_2$  microstructurally modified by ball milling: study performed with different physicochemical  $\text{CO}_2$  capture conditions, *RSC Adv.* 6 (2016) 57880–57888.
- [32] H.A. Lara-García, E. Vera, J.A. Mendoza-Nieto, J.F. Gómez-García, Y. Duan, H. Pfeiffer, Bifunctional application of lithium ferrites ( $\text{Li}_5\text{FeO}_4$  and  $\text{LiFeO}_2$ ) during carbon monoxide ( $\text{CO}$ ) oxidation and chemisorption processes. A catalytic, thermogravimetric and theoretical analysis, *Chem. Eng. J.* 313 (2017) 1288–1294.
- [33] Y. Matsukura, T. Okumura, R. Kobayashi, K. Oh-Ishi, Synthesis and  $\text{CO}_2$  absorption properties of single-phase  $\text{Li}_2\text{CuO}_2$  as a  $\text{CO}_2$  absorbent, *Chem. Lett.* 39 (2010) 966–967.
- [34] K. Oh-Ishi, Y. Matsukura, T. Okumura, Y. Matsunaga, R. Kobayashi, Fundamental research on gas-solid reaction between  $\text{CO}_2$  and  $\text{Li}_2\text{CuO}_2$  linking application for solid  $\text{CO}_2$  absorbent, *J. Solid State Chem.* 211 (2014) 162–169.
- [35] L.M. Palacios-Romero, H. Pfeiffer, Lithium cuprate ( $\text{Li}_2\text{CuO}_2$ ): A new possible ceramic material for  $\text{CO}_2$  chemisorption, *Chem. Lett.* 37 (2008) 862–863.
- [36] L.M. Palacios-Romero, E. Lima, H. Pfeiffer, Structural analysis and  $\text{CO}_2$  chemisorption study on nonstoichiometric lithium cuprate ( $\text{Li}_2 + x\text{CuO}_2 + x/2$ ), *J. Phys. Chem. A* 113 (2009) 193–198.
- [37] F. Sapiña, J. Rodríguez-Carvajal, M.J. Sanchis, R. Ibañez, A. Beltran, D. Beltran, Crystal and magnetic structure of  $\text{Li}_2\text{CuO}_2$ , *Solid State Commun.* 74 (1990) 779–784.
- [38] J.W. Kim, H.G. Lee, Thermal and carbothermic decomposition of  $\text{Na}_2\text{CO}_3$  and  $\text{Li}_2\text{CO}_3$ , *Metall. Mater. Trans. B* 32 (2001) 17–24.
- [39] J.W. Kim, Y.D. Lee, H.G. Lee, Decomposition of  $\text{Li}_2\text{CO}_3$  by interaction with  $\text{SiO}_2$  in mold flux of steel continuous casting, *ISIJ Int.* 44 (2004) 334–341.